

Predicted band-gap pressure coefficients of all diamond and zinc-blende semiconductors: Chemical trends

Su-Huai Wei and Alex Zunger

National Renewable Energy Laboratory, Golden, Colorado 80401

(Received 25 February 1999)

We have studied systematically the chemical trends of the band-gap pressure coefficients of all group IV, III-V, and II-VI semiconductors using first-principles band-structure method. We have also calculated the individual ‘‘absolute’’ deformation potentials of the valence-band maximum (VBM) and conduction-band minimum (CBM). We find that (1) the volume deformation potentials of the Γ_{6c} CBM are usually large and always negative, while (2) the volume deformation potentials of the Γ_{8v} VBM state are usually small and negative for compounds containing occupied valence d state but positive for compounds without occupied valence d orbitals. Regarding the chemical trends of the band-gap pressure coefficients, we find that (3) $a_p^{\Gamma-\Gamma}$ decreases as the ionicity increases (e.g., from Ge \rightarrow GaAs \rightarrow ZnSe), (4) $a_p^{\Gamma-\Gamma}$ increases significantly as anion atomic number increases (e.g., from GaN \rightarrow GaP \rightarrow GaAs \rightarrow GaSb), (5) $a_p^{\Gamma-\Gamma}$ decreases slightly as cation atomic number increases (e.g., from AlAs \rightarrow GaAs \rightarrow InAs), (6) the variation of $a_p^{\Gamma-L}$ are relatively small and follow similar trends as $a_p^{\Gamma-\Gamma}$, and (7) the magnitude of $a_p^{\Gamma-X}$ are small and usually negative, but are sometimes slightly positive for compounds containing first-row elements. Our calculated chemical trends are explained in terms of the energy levels of the atomic valence orbitals and coupling between these orbital. In light of the above, we suggest that ‘‘empirical rule’’ of the pressure coefficients should be modified. [S0163-1829(99)00532-9]

I. INTRODUCTION

The pressure (p) coefficient

$$a_p^\alpha = \frac{dE_\alpha}{dp} \quad (1)$$

of an interband transition α (e.g., $\Gamma_{8v} \rightarrow \Gamma_{6c}$, $\Gamma_{8v} \rightarrow L_{6c}$, $\Gamma_{8v} \rightarrow X_{6c}$) in a semiconductor is related to the volume (v) deformation potential

$$a_v^\alpha = \frac{dE_\alpha}{d \ln v} \quad (2)$$

via the bulk modulus $B = -dp/d \ln v$ through the relation

$$a_p^\alpha = -\left(\frac{1}{B}\right) a_v^\alpha. \quad (3)$$

For semiconductors with the diamond and zinc-blende structures, the accumulated knowledge distilled from many measurements of a_p^α for the main interband transitions were summarized by William Paul^{1,2} in the ‘‘empirical rules of the pressure coefficients,’’ namely that for a fixed interband transition type α , the pressure coefficient a_p^α is nearly constant for all tetrahedral semiconductors; the main dependence is on the transition type α . For $\alpha = \Gamma_{8v} \rightarrow \Gamma_{6c}$ transition $a_p^{\Gamma-\Gamma}$ is of the order of 10 meV/kbar, for $\alpha = \Gamma_{8v} \rightarrow L_{6c}$ transition $a_p^{\Gamma-\Gamma}$ is near 5 meV/kbar, and for $\alpha = \Gamma_{8v} \rightarrow X_{6c}$ transition $a_p^{\Gamma-X}$ is around -1 or -2 meV/kbar. This ‘‘empirical rule’’ has been used successfully in the past to identify from high-pressure optical experiment the symmetry of optical transitions in semiconductors²⁻⁴ and to determine the band offset

at zinc-blende semiconductor interfaces.⁵ However, a closer look at the currently available experimental data⁶⁻¹³ indicates that the validity of the ‘‘empirical rule’’ is rather questionable. For example, the pressure coefficient of $a_p^{\Gamma-\Gamma}$ changes significantly with anion, from ~ 4 meV/kbar for GaN to ~ 10 meV/kbar for GaP to ~ 14 meV/kbar for GaSb. Since, however, the available experimental pressure coefficients a_p sometimes have a large spread, it is difficult to assess the chemical trends of the pressure coefficients without either a systematic measurements or systematic calculations.

The other issue in this field is to determine how much of the band-gap deformation a_p^α comes from the valence band and how much comes from the conduction band.¹⁴⁻¹⁷ This information is crucial in assessing quantum confinement for holes, and separately for electrons in heterostructure. It is customary^{18,19} to assumed that the volume deformation potentials a_v^{VBM} of the valence-band maximum (VBM) state Γ_{8v} are positive, i.e., that the energy of the VBM state *decreases* as the volume decreases. This is based on the argument that the VBM state is a ‘‘bonding’’ state of anion p and cation p orbitals.²⁰ However, assuming the deep impurity pinning rule,²¹ experimental measurements^{22,23} find that a_v^{VBM} are negative for the III-V semiconductors GaAs and InP. Theoretical calculations of the absolute deformation potentials also give contradictory results. For example, using dielectric midgap energy model Cardona and Christensen¹⁵ find that a_v^{VBM} is always *negative*, while using the model-solid theory, Van de Walle¹⁶ finds that a_v^{VBM} is always *positive*.

In this paper, we test the validity of the ‘‘empirical rule’’ and study the *chemical trends* of the band-gap pressure co-

efficients by systematically calculating the pressure coefficients for all group IV, III-V, and II-VI semiconductors. We also calculate the “absolute” deformation potentials of the VBM and conduction-band maximum (CBM). We show that (1) the volume deformation potentials a_v^{CBM} of the conduction-band minimum (CBM) state Γ_{6c} are usually large and always negative (energy increases with pressure), while (2) the volume deformation potentials a_v^{VBM} of the VBM Γ_{8v} state are usually small and negative for zinc-blende compounds containing occupied valence d state (e.g., GaAs, InAs) but positive for compounds without occupied valence d orbitals (e.g., AlAs). Regarding the chemical trends of the band-gap pressure coefficients, we find that (3) $a_p^{\Gamma-\Gamma}$ decreases as the ionicity increases, (4) $a_p^{\Gamma-\Gamma}$ increases significantly as anion atomic number increases, (5) $a_p^{\Gamma-\Gamma}$ decreases slightly as cation atomic number increases, (6) the variation of $a_p^{\Gamma-L}$ are relatively small and follow similar trends as $a_p^{\Gamma-\Gamma}$, and (7) the magnitude of $a_p^{\Gamma-X}$ are small and usually negative, but are positive for compounds containing first row elements (C, AlN, GaN, InN, etc.). Our calculated chemical trends can be understood using the $s-s$ and $s-d$ coupling models for the conduction states and $p-p$ and $p-d$ coupling models for the VBM. In light of the above noted chemical trends, we suggest that the “empirical rule”^{1,2} of the pressure coefficients should be modified and that one should be cautious in using the absolute deformation potentials from previous calculations.^{15,16}

II. METHOD OF CALCULATION

We calculate the band-gap pressure coefficient [Eq. (1)] via self-consistent local density approximation (LDA),²⁴ as implemented by the relativistic, linearized augmented plane-wave (LAPW) method.²⁵ We used the Ceperley-Alder exchange correlation potential²⁶ as parameterized by Perdew and Zunger.²⁷ The Ga $3d$, In $4d$, Zn $3d$, Cd $4d$, and Hg $5d$, states are treated in the same footing as the other s and p valence states. A well-converged basis set of about 300 LAPW's per atom is used. The Brillouin-zone summation is performed using ten special²⁸ k points. To obtain the band-gap pressure coefficient a_p^α , we first calculate the volume deformation potential a_v^α [Eq. (2)] at the experimental lattice constant and then calculate the bulk modulus by fitting the calculated total energy to the Murnahan's equation of states,²⁹ which assumes

$$B(p) = B(0) + B'p, \quad (4)$$

where B' is the pressure derivative of the bulk modulus. The band-gap pressure coefficient is then obtained from a_v^α and B using Eq. (3). To obtain the “absolute deformation potential” of the valence-band maximum state, we calculate the deformation potential of the transition between the VBM and the averaged cation and anion $1s$ core levels. We approximate that the cation-anion average of the absolute deformation potential of the localized $1s$ core state is negligible. The uncertainty due to this approximation is about ± 0.5 meV/kbar.¹⁷

Before we study the chemical trends, we tested two common assumptions used in measuring the pressure coefficient.

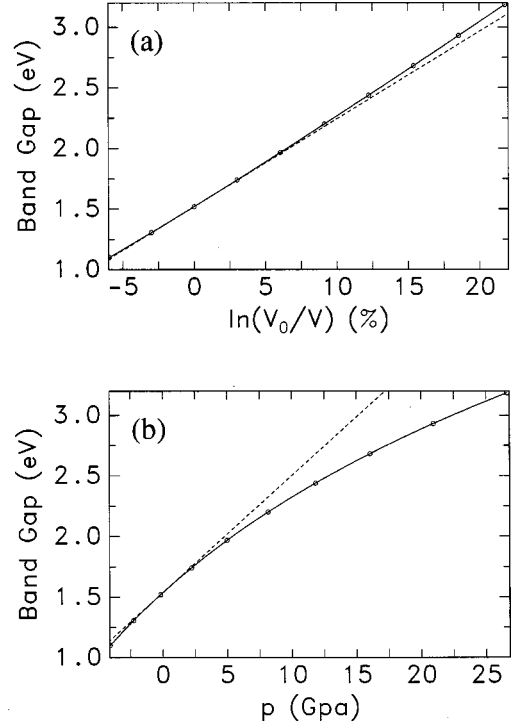


FIG. 1. Calculated direct band gap at Γ for GaAs as (a) a function of $\ln v$ and (b) a function of p . The dashed lines are linear function predictions using the values and slopes at $p=0$. A constant is added to the band gap E_g so it equals to experimental value at $p=0$.

(a) Is E_g linear with p or with $\ln v$? It is customary to assume that the direct band gap E_g is a linear function of either the relative volume change $\ln v$ or the pressure p . Equations (3) and (4) imply that it cannot both be right since B' is known to be positive,⁶ i.e., the bulk modulus increases significantly as volume decreases. Figure 1 shows our calculated E_g for GaAs as a function of $\ln v$ as well as a function of p . We see from Fig. 1 that to a good approximation E_g is a linear function of $\ln v$, but not a linear function of p . Indeed, dE_g/dp decreases as p increases, while $-dE_g/d \ln v$ increases only slightly as the volume decreases. This conclusion is consistent with experimental observations.^{7,30}

At low pressure, one can fit $E_g(p)$ to a quadratic function

$$E_g(p) = E_g(0) + \alpha p + \beta p^2. \quad (5)$$

Using Eqs. (3) and (4), we find that β/α is bounded by

$$0 < -\beta/\alpha \leq B'/2B(0). \quad (6)$$

For InP the measured values^{30,31} $-\beta/\alpha = 0.002$ kbar⁻¹, which is within the bound of 0 to 0.0034 kbar⁻¹ obtained from Eq. (6). We find, however, that using Eq. (5) the fitted values α and β depend sensitively on the pressure range used in the fitting. For GaAs, α and β values obtained using data between $p=0$ to $p=200$ kbar is about 5% and 50%, respectively, smaller than the values obtained by fitting the data near $p=0$. If one fits to a linear equation [i.e., set $\beta=0$ in Eq. (5)] α obtained using data between $p=0$ to $p=200$ kbar is almost 30% smaller than the value obtained by fitting the data near $p=0$.

(b) Does $a_p^{\Gamma-\Gamma}$ depend on whether it is zinc-blende or wurtzite structure? In our calculation we used the cubic diamond or zinc-blende (ZB) structure to obtain the pressure

TABLE I. Comparison of LDA-calculated band-gap pressure coefficients (in meV/kbar) for the nitrides in the zinc-blende (ZB) and wurtzite (WZ) structures. The values for the WZ structure are averaged over the crystal-field split VBM states. The differences between the crystal-field split values is less than 0.1 meV/kbar.

Compound	$a_p^\Gamma(\text{ZB})$	$a_p^\Gamma(\text{WZ})$
AlN	4.2	4.3
GaN	3.1	3.3
InN	1.8	2.1

coefficients for all the compounds. However, the stable crystal structures for the nitrides and some of the II-VI compounds (CdS, CdSe) are wurtzite (WZ). It appears reasonable to assume that compounds in the WZ structure will have similar pressure coefficients as in the ZB structure, since the nearest-neighbor tetrahedral environment is similar in both structures. However, a recent calculation of Christensen *et al.*³² using linearized muffin-tin orbital (LMTO) method found that for InN $a_p^{\Gamma-\Gamma} = 3.1$ meV/kbar in the WZ structure, but only 1.9 meV/kbar in the ZB structure. The difference was attributed to the extra structural degrees of freedom available in the WZ structure: the variation of E_g due to the change in the $\eta = c/a$ ratio (where c and a are the hexagonal lattice constants parallel and perpendicular to the $[0001]$ direction), and the internal structural parameter u . To test their results, we have repeated their calculation for InN. In the WZ structure

$$\frac{dE_g}{d \ln v} = \frac{\partial E_g}{\partial \ln v} + \frac{\partial E_g}{\partial \eta} \frac{\partial \eta}{\partial \ln v} + \frac{\partial E_g}{\partial u} \frac{\partial u}{\partial \ln v}, \quad (7)$$

where all the quantities are calculated near equilibrium. We find that for WZ-InN $\partial \eta / \partial \ln v = -0.001$ and $\partial u / \partial \ln v = 0.030$ are both very small (they are, of course, equal to zero for ZB structure), thus the contribution of the last two terms in Eq. (7) to $dE_g / d \ln v$ accounts less than 2%. The calculated bulk moduli (1498 kbar for the ZB structure and 1484 kbar for the WZ structure) are similar in both structures. Thus, the main difference between the ZB and WZ structures are due to the terms $\partial E_g / \partial \ln v$ in Eq. (7). Table I compares the LDA calculated pressure coefficients for AlN, GaN, and InN in the zinc-blende and the wurtzite structures. We see that the pressure coefficient is only 0.3 meV/kbar or less larger in the wurtzite structure than in the zinc-blende structure. For ZB-InN, we find $a_p^{\Gamma-\Gamma} = 1.8$ meV/kbar is in good agreement with Christensen *et al.*'s results $a_p^{\Gamma-\Gamma} = 1.9$ meV/kbar, but for WZ-InN we find $a_p^{\Gamma-\Gamma} = 2.1$ meV/kbar, much smaller than the 3.1 meV/kbar value of Christensen *et al.* The difference between our calculated pressure coefficient for WZ-InN and that of Christensen *et al.*³² is not understood. We will use zinc-blende structure only in our following calculations.

III. CALCULATED VALUES AND EMERGING TRENDS

Table II gives the LDA calculated equilibrium lattice constants a , bulk moduli B , and pressure derivative B' of the bulk modulus. We find that our calculated lattice constants

TABLE II. LDA-calculated (cal) equilibrium zinc-blende lattice constants a (in Å), bulk moduli B (in kbar), and the pressure derivative B' of the bulk modulus. Results are compared with available experimental (exp) data (Ref. 6). Compounds denoted by an asterisk exist in wurtzite structure, while HgS exist in the cinnabar structure. For these compounds a_{exp} and B_{exp} are estimated from the properties of their wurtzite counterpart or from LDA calculations.

Compound	a_{cal}	a_{exp}	B_{cal}	B_{exp}	B'_{cal}
C	3.5393	3.5668	4692	4420	3.8
Si	5.4069	5.4307	966	979	4.4
Ge	5.6540	5.6579	708	689	4.5
Sn	6.5029	6.4890	443	456	4.6
AlN*	4.3641	4.3600	2158	2158	4.2
AlP	5.4461	5.4635	903	860	4.4
AlAs	5.6435	5.6600	754	781	4.4
AlSb	6.1234	6.1355	560	551	4.4
GaN*	4.4881	4.5000	2063	2054	4.6
GaP	5.4374	5.4505	896	882	4.7
GaAs	5.6490	5.6533	742	756	4.8
GaSb	6.0917	6.0959	556	563	4.9
InN*	4.9753	4.9800	1498	1480	4.7
InP	5.8615	5.8687	716	710	4.8
InAs	6.0512	6.0583	603	579	4.9
InSb	6.4763	6.4794	468	483	4.9
ZnS	5.3476	5.4102	906	771	5.0
ZnSe	5.6079	5.6676	740	624	5.0
ZnTe	6.0295	6.0890	559	509	5.1
CdS*	5.7958	5.8180	703	620	4.8
CdSe*	6.0412	6.0520	592	530	4.8
CdTe	6.4400	6.4820	466	445	4.9
HgS	5.8476	5.8500	689	685	5.0
HgSe	6.0950	6.0850	589	500	5.0
HgTe	6.4677	6.4603	477	423	5.1

and bulk moduli agree very well with experimental data,⁶ especially for III-V compounds. The LDA error for the lattice constants and bulk moduli are somewhat larger for the II-VI Zn compounds.

Table III gives the LDA-calculated band-gap deformation potentials and pressure coefficients of the three main transitions $\Gamma_{8v} \rightarrow X_{6c}$, $\Gamma_{8v} \rightarrow L_{6c}$, and $\Gamma_{8v} \rightarrow \Gamma_{6c}$. Comparing to experimental data, we find that the calculated band-gap pressure coefficients $a_p^{\Gamma-\Gamma}$ are *systematically* $\sim 1-2$ meV/kbar smaller than the experimental values. The error seems to be larger for compounds with smaller band gaps. However, since the LDA errors are *systematic* (see discussion in Sec. VI on LDA corrections), the *trends* of the band gap pressure coefficient are well reproduced in the LDA calculation. We find that (i) $a_p^{\Gamma-\Gamma}$ decreases as the ionicity increases, e.g., from Ge \rightarrow GaAs \rightarrow ZnSe, (ii) $a_p^{\Gamma-\Gamma}$ increases significantly as the anion atomic number increases, e.g., from GaN \rightarrow GaP \rightarrow GaAs \rightarrow GaSb, (iii) $a_p^{\Gamma-\Gamma}$ decreases slightly as cation atomic number increases, e.g., from AlAs \rightarrow GaAs \rightarrow InAs, (iv) the variation of $a_p^{\Gamma-L}$ are relatively small and follow similar trends as $a_p^{\Gamma-\Gamma}$, and (v) the magnitude of $a_p^{\Gamma-X}$ are small; $a_p^{\Gamma-X}$ are usually negative, but are positive for compounds containing first-row elements

TABLE III. LDA-Calculated band-gap volume deformation potentials [Eq. (2)] (in eV) and pressure coefficient [Eq. (1)] (in meV/kbar) of the three main transitions $\Gamma_{8v} \rightarrow X_{6c}$, $\Gamma_{8v} \rightarrow L_{6c}$, and $\Gamma_{8v} \rightarrow \Gamma_{6c}$ for group IV, III-V, and II-VI semiconductors. Results for $a_p^{\Gamma-\Gamma}$ are compared with available experimental (exp) data (Ref. 6, unless specified otherwise).

Compound	$a_v^{\Gamma-X}$	$a_p^{\Gamma-X}$	$a_v^{\Gamma-L}$	$a_p^{\Gamma-L}$	$a_v^{\Gamma-\Gamma}$	$a_p^{\Gamma-\Gamma}$	$a_p^{\Gamma-\Gamma}$ (exp)
C	-2.31	0.49	-13.65	2.91	-23.08	4.9	
Si	1.84	-1.90	-3.60	3.73	-11.39	11.8	
Ge	1.16	-1.64	-3.07	4.34	-9.10	12.9	
Sn	0.97	-2.19	-1.96	4.42	-6.97	15.7	
AlN	-0.42	0.19	-9.04	4.11	-9.04	4.2	
AlP	1.86	-2.06	-3.77	4.17	-8.50	9.4	
AlAs	1.63	-2.16	-3.77	5.00	-7.86	10.4	10.2
AlSb	1.71	-3.05	-2.90	5.18	-7.85	14.0	
GaN	-0.35	0.17	-6.72	3.26	-6.40	3.1	4.0 ^a
GaP	1.97	-2.20	-2.96	3.30	-7.99	8.9	9.7
GaAs	1.81	-2.44	-2.66	3.58	-7.25	9.8	8.5–12.6
GaSb	1.80	-3.24	-2.04	3.67	-7.01	12.6	14.0
InN	-0.45	0.30	-3.97	2.65	-2.75	1.8	
InP	1.62	-2.26	-2.25	3.14	-5.30	7.4	8.0; 7.5–9.3 ^b
InAs	1.58	-2.62	-1.98	3.28	-4.93	8.2	11.4; 9.6–11.4 ^b
InSb	1.66	-3.55	-1.65	3.53	-5.60	12.0	12.8–15.5
ZnS	2.10	-2.32	-1.97	2.17	-4.28	4.7	5.8; 6.4 ^c ; 6.7 ^d
ZnSe	2.16	-2.92	-1.74	2.35	-3.96	5.4	7.2–7.5; 7.0 ^c
ZnTe	2.42	-4.33	-1.31	2.34	-4.67	8.4	11.5; 10.5 ^e
CdS	1.62	-2.30	-1.38	1.96	-2.08	3.0	4.4; 4.6 ^c
CdSe	1.81	-3.05	-1.17	1.98	-1.96	3.3	5.8
CdTe	2.09	-4.48	-0.98	2.10	-2.95	6.3	7.6 ^e ; 6.5–8.6 ^f
HgS	1.91	-2.77	-0.34	0.49	-1.23	1.8	
HgSe	2.20	-3.74	-0.06	0.10	-1.15	2.0	
HgTe	2.49	-5.22	-0.01	0.02	-2.34	4.9	

^aReference 8.

^bReference 9.

^cReference 10.

^dReference 11.

^eReference 12.

^fReference 13.

(C, AlN, GaN, InN, etc.). In the following, we will analyze the chemical trends of the volume deformation potentials and pressure coefficients in terms of simple models, including the $s-s$, $p-p$, and $p-d$ couplings and level repulsions.

IV. EXPLANATION OF TRENDS USING SIMPLE MODELS

Since the deformation potential $a_v^{\Gamma-\Gamma} = a_v^{\text{CBM}} - a_v^{\text{VBM}}$, where $a_v^{\text{CBM}} = dE^{\text{CBM}}/d \ln v$ is the deformation potential of the CBM (Γ_{6c}) and $a_v^{\text{VBM}} = dE^{\text{VBM}}/d \ln v$ is the deformation potential of VBM (Γ_{8v}), we will first analyze individually the chemical trends of the CBM and VBM volume deformation potentials (Table IV) and the volume dependence of the bulk moduli (Table II):

A. Volume deformation potential of the Γ_{6c} state

Under pressure, the antibonding Γ_{6c} state moves upward in energy due to (a) increase in the kinetic energy, which is proportional to k^2 or $1/l^2$, where k is the reciprocal lattice vector (in the extended Brillouin zone) and l is the anion-cation bond length, and (b) $s-s$ level repulsion. The two effects add up for this antibonding state, so a_v^{CBM} is always positive and mostly large. The variation of a_v^{CBM} due to the

$s-s$ level repulsion can be modeled approximately using the simple tight-binding model²⁰ where

$$E^{\text{CBM}} = \frac{\epsilon_s^c + \epsilon_s^a}{2} + \sqrt{\left(\frac{\epsilon_s^c - \epsilon_s^a}{2}\right)^2 + V_{ss}^2}. \quad (8)$$

Here, ϵ_s^c and ϵ_s^a are cation and anion s orbital energies, respectively, and the coupling potential between cation s and anion s states V_{ss} varies approximately as $\sim b_{ss}/l^2$, where b_{ss} is a compound-dependent constant. Taking a derivative with respect to volume $v \propto l^3$, we find that the contribution of $s-s$ coupling to the deformation potential is

$$a_v^{\text{CBM}}(ss) = \frac{-4b_{ss}^2}{3l^2[(\epsilon_s^c - \epsilon_s^a)^2 l^4 + 4b_{ss}^2]^{1/2}}. \quad (9)$$

(1) In the homopolar limit where $\epsilon_s^c = \epsilon_s^a$, Eq. (9) is reduced to $a_v^{\text{CBM}}(ss) = -2b_{ss}/3l^2$, thus the magnitude of a_v^{CBM} is expected to increase as the bondlengths of the covalent compounds decrease. This explains why $-a_v^{\text{CBM}}(\text{C}) = 20.53$ eV is so much larger than $-a_v^{\text{CBM}}(\text{Sn}) = 7.89$ eV.

(2) In the ionic limit $a_v^{\text{CBM}}(ss) \approx -4b_{ss}/[3l^4(\epsilon_s^c - \epsilon_s^a)]$, i.e., inversely proportional to the energy difference between the cation s orbitals and anion s orbitals.

TABLE IV. LDA-Calculated “absolute” volume deformation potentials (in eV) of the VBM (Γ_{8v}) and the CBM (Γ_{6c}) states at Γ for group IV, III-V, and II-VI semiconductors.

Compound	a_v^{VBM}	a_v^{CBM}
C	2.55	-20.53
Si	2.05	-9.34
Ge	-0.35	-9.45
Sn	-0.92	-7.89
AlN	4.94	-4.10
AlP	2.64	-5.86
AlAs	1.53	-6.33
AlSb	0.73	-7.12
GaN	0.69	-5.71
GaP	-0.58	-8.57
GaAs	-1.21	-8.46
GaSb	-1.32	-8.33
InN	0.73	-2.02
InP	-0.41	-5.71
InAs	-1.00	-5.93
InSe	-1.24	-6.84
ZnS	-1.74	-6.02
ZnSe	-1.97	-5.93
ZnTe	-2.28	-6.95
CdS	-1.51	-3.59
CdSe	-1.81	-3.77
CdTe	-2.14	-5.09
HgS	-3.06	-4.29
HgSe	-3.20	-4.35
HgTe	-3.45	-5.79

(3) For the *common-cation* system, since $\epsilon_s^c - \epsilon_s^a$ usually decrease as anion-atomic number increases (Fig. 2), Eq. (9) show that a_v^{CBM} tend to be larger for heavier anion compounds. This effect, however, is partially cancelled by the increase in the bondlength when the anion-atomic number increases. The net effect is that a_v^{CBM} has a relatively small variations with anion for common-cation system. The relatively big jump in a_v^{CBM} between nitride and phosphide ($\Delta a_v^{\text{CBM}} = 1.76$ eV for AlX, 2.86 for GaX, and 3.69 for InX, X=N or P) are attributed to the large energy differences (Fig. 2) between N 2s and P 3s orbitals (4.4 eV). The same arguments explains why Te compounds have larger a_v^{CBM} than Se compounds since Te 5s orbital energy is 2.1 eV higher than Se 4s orbital energy (Fig. 2).

(4) For the *common-anion* system, the change in cation valence s orbital energy is not a monotonic function of the atomic number of cations in the same column of the Periodic Table (Fig. 2). For example, due to the incomplete screening of the valence d orbitals,^{33,34} the Ga 4s orbital energy is 1.3 eV lower than the Al 3s orbital energy and 0.7 eV lower than the In 5s orbital energy. As a result, the magnitude of a_v^{CBM} for GaX (X=N, P, As, and Sb) are larger than AlX, even though they have similar bond lengths. The larger $|a_v^{\text{CBM}}|$ for AlX than for InX is due to the smaller bondlengths of AlX. The same argument explains why HgX (X=S, Se, Te) compounds has larger $|a_v^{\text{CBM}}|$ than CdX even though they have similar bondlengths: Due to relativistic ef-

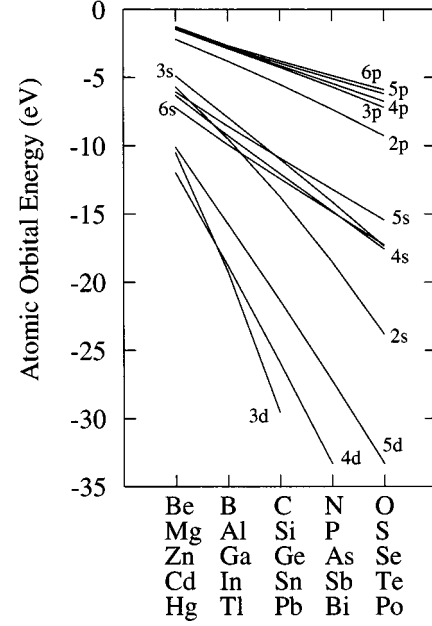


FIG. 2. LDA-calculated valence atomic energy levels. Lines are used to guide eyes.-

fects, the Hg 6s orbital energy is 1.2 eV lower than Cd 5s orbital energy (Fig. 2).

B. Volume deformation potential of the Γ_{8v} state

The change of the VBM states under pressure are due to the following three effects. (a) The kinetic energy effect, which moves the energy of the VBM higher under pressure. (b) The anion-cation $p-p$ coupling effect, which lowers the energy of the VBM under pressure, since the VBM is a $p-p$ bonding state. The $p-p$ coupling increases with decreasing bondlength l and decreasing energy difference between the cation p and anion p orbital energies ($\epsilon_p^c - \epsilon_p^a$). Effects (a) and (b) partially cancel each other, so a_v^{VBM} are usually much smaller than a_v^{CBM} . (c) For compounds that have active d valence bands, there is also a $p-d$ coupling effect,^{33,34} which is often neglected in previous calculations.^{20,16} This coupling exist because in tetrahedral coordinated compounds, the p orbital and the d orbital have the same representation at Γ (Γ_{15v} or $\Gamma_{25'v}$) thus they can couple and repel each other. Since the VBM is a $p-d$ anti-bonding state when cation valence d orbital energy is below the anion p orbital energy, $p-d$ coupling for these compounds make the energy of the VBM higher under pressure. The $p-d$ coupling increases with decreasing bondlength l and decreasing energy difference between the cation d and anion p orbital energies ($\epsilon_d^c - \epsilon_p^a$).

We find that (1) a_v^{VBM} decreases with anion atomic number due to the increase of the bond length. (2) Due to the $p-d$ repulsion effect, a_v^{VBM} are negative for GaX and InX (X=P, As, and Sb) and for ZnX, CdX, and HgX (X=S, Se, and Te). (3) a_v^{VBM} are more negative for II-VI compounds where $p-d$ repulsion effect are large.

Our finding of negative a_v^{VBM} contradicts to common believe that a_v^{VBM} is always positive.^{20,16} However, our calcu-

lated results of $a_v^{\text{VBM}}(\text{GaAs}) = -1.21 \text{ eV}$ and $a_v^{\text{VBM}}(\text{InP}) = -0.41 \text{ eV}$ are consistent with experimental observation of -1.0 and -0.6 eV for GaAs (Ref. 23) and InP,²² assuming deep-defect level pinning rule.²¹ Our results differ from Van de Walle's model solid theory calculation¹⁶ where all the a_v^{VBM} are found to be positive. Our results also differ from the LMTO calculation of Cardona and Christensen, which apply the dielectric midgap energy model. They find that a_v^{VBM} are always negative, even for AlX and Si. Our calculated a_v^{VBM} for Si is 2.05 eV, similar to the $\sim 2.2 \text{ eV}$ value derived from (110) interfacial strain,^{17,35,36} but differ from the -1.6 eV value from the LMTO calculation.^{15,37} Our calculated a_v^{VBM} for ZnS (-1.74 eV) is also much smaller in magnitude than the LMTO results (-4.10 eV).

C. Bulk moduli of semiconductor compounds

Cohen and coworkers³⁸ have show that the bulk moduli of the semiconductor compounds follow a simple power law

$$B = kl^{-n}, \quad (10)$$

where k is nearly a constant and n is close to 3.5, increases slightly as the ionicity increases. Since for the diamond compounds the decrease in magnitude of $a_p^{\Gamma-\Gamma}$ as a function of bond length l is in the order of $\sim l^{-2}$ [Eq. (9)], slower than the decrease of the bulk modulus B , $a_p^{\Gamma-\Gamma}$ is expected to increase with atomic number for group-IV elements. Indeed we find the pressure coefficients increase from 4.9 meV/kbar for C to 15.7 meV/kbar for Sn.

D. Chemical trends in the pressure coefficient

Our analysis above indicate that $s-s$ and $p-p$ coupling enhance the pressure coefficient $a_p^{\Gamma-\Gamma}$, while the $p-d$ coupling reduces the pressure coefficient. The fast reduction of the bulk modulus as the bondlength increases enhances the pressure coefficients of compounds with large atomic size. Using these simple rules, we can explain the chemical trends observed from our calculation of the pressure coefficient of zinc-blende compounds:

(i) $a_p^{\Gamma-\Gamma}$ decreases with increasing ionicity. For example, the LDA calculated $a_p^{\Gamma-\Gamma}$ are 12.9, 9.8, and 5.4 meV/kbar for Ge, GaAs, and ZnSe, which have similar bondlengths. This trend reflects two effects: *First*, the cation-anion $s-s$ coupling decreases as the ionicity increases, since $\epsilon_s^c - \epsilon_s^a$ increases. *Second*, the cation-anion $p-d$ coupling increases as ionicity increases, thus reduces $a_p^{\Gamma-\Gamma}$.

(ii) $a_p^{\Gamma-\Gamma}$ increases significantly when the anion-atomic number increases. For example, the LDA calculated $a_p^{\Gamma-\Gamma}$ are 3.1, 8.9, 9.8, and 12.6 meV/kbar for GaN, GaP, GaAs, and GaSb, respectively. In this case, the increase in $a_p^{\Gamma-\Gamma}$ is mainly due to the large decrease in bulk moduli when anion-atomic number increases. The large increases in the pressure coefficient from nitrides to phosphides and from As to Sb in III-V compounds or from selenides to tellurides in II-VI compounds are also caused by enhanced $s-s$ and $p-p$ coupling, since $\epsilon_s^c - \epsilon_s^a$ and $\epsilon_s^c - \epsilon_s^a$ decrease as anion-atomic number increases.

(iii) $a_p^{\Gamma-\Gamma}$ decreases slightly when the cation-atomic number increases. For example, the LDA calculated $a_p^{\Gamma-\Gamma}$ are

10.4, 9.8, and 8.2 meV/kbar for AlAs, GaAs, and InAs, respectively. Comparing AlAs with GaAs, which has similar lattice constants and bulk moduli, we find that GaAs has large $s-s$ coupling due to its smaller $\epsilon_s^c - \epsilon_s^a$ energy difference, but it also has larger $p-d$ coupling. The net effect is that $a_p^{\Gamma-\Gamma}$ for AlAs is slightly larger than for GaAs. Comparing GaAs with InAs, we notice that $p-d$ coupling in both compounds are similar but the $s-s$ coupling is much larger in GaAs than in InAs, due to the smaller $\epsilon_s^c - \epsilon_s^a$ energy difference and shorter bondlength in GaAs. However, the bulk modulus of InAs is smaller than GaAs, due to its larger lattice constant [Eq. (10)]. The net effect is that $a_p^{\Gamma-\Gamma}$ for InAs is reduced but only slightly relative to GaAs. Similar trends are found for other common-anion system, i.e., $a_p^{\Gamma-\Gamma}$ decreases with increasing cation-atomic numbers. However, due to the cancellation of various effects, the change in $a_p^{\Gamma-\Gamma}$ for common-anion system is relatively small comparing to common-cation system.

(iv) We find that $a_p^{\Gamma-L}$ has similar trends as $a_p^{\Gamma-\Gamma}$, but the variation is smaller. The small variation in $a_p^{\Gamma-L}$ is due to the more complete cancellation between the reduced level repulsion and the reduced bulk modulus as bondlength increases.

(v) We find that $a_p^{\Gamma-X}$ for the $\Gamma_{8v} \rightarrow X_{6c}$ transition is usually small and negative, as predicted by the ‘‘empirical rule.’’^{1,2} The negative pressure coefficient $a_p^{\Gamma-X}$ is due to (a) the level repulsion between the X_{6c} state and unoccupied d state (e.g., $3d$ state in Si or AlP) with the same principle quantum number as the valence s and p state,³⁹ and/or (b) large $p-d$ repulsion of occupied states at the VBM. However, contrary to the empirical rule, we find that some of the compounds (C, AlN, GaN, and InN) have positive $a_p^{\Gamma-X}$. The reason that C, GaN, InN have positive $a_p^{\Gamma-X}$ is mainly due to lack of (a), while the reason AlN has positive $a_p^{\Gamma-X}$ is mainly due to lack of (b). Our LDA calculated $a_p^{\Gamma-X} = 0.49 \text{ meV/kbar}$ for C is consistent with experimental value of $\sim 0.5 \text{ meV/kbar}$ and the calculated results of Fahy *et al.* ($\sim 0.55 \text{ meV/kbar}$).³⁹

V. COMPARISON WITH EXPERIMENT

Our predicted chemical trends is consistent with most experimental data (Table III). However, there are some exceptions. For example, using linear composition-dependence assumption, Adachi¹⁹ estimated that the pressure coefficient $a_p^{\Gamma-\Gamma}$ for $\text{Al}_x\text{Ga}_{1-x}\text{As}$ is 11.5-1.3x meV/kbar, i.e., for pure AlAs ($x=1$) its pressure coefficient is 1.3 meV/kbar smaller than GaAs. Our calculation, however, find that $a_p^{\Gamma-\Gamma}$ for AlAs is about 0.6 meV/kbar higher than that for GaAs. We believe that the discrepancy between our theory and experiment¹⁹ is due to the linear composition dependence assumption used in the experiment. To test this, we have calculated the band-gap pressure coefficient $a_p^{\Gamma-\Gamma}(x)$ for random $\text{Al}_{0.5}\text{Ga}_{0.5}\text{As}$ alloy using the special quasirandom structure approach.⁴⁰ The calculated results are fitted to a quadratic function

$$a_p^{\Gamma-\Gamma}(x) = (1-x)a_p^{\Gamma-\Gamma}(\text{GaAs}) + xa_p^{\Gamma-\Gamma}(\text{AlAs}) - b_p^{\Gamma-\Gamma}x(1-x), \quad (11)$$

where the bowing coefficient $b_p^{\Gamma-\Gamma}$ of the pressure coefficient is found to be 3.8 meV/kbar for $\text{Al}_x\text{Ga}_{1-x}\text{As}$. Since $b_p^{\Gamma-\Gamma}$ is larger than the difference (0.6 meV/kbar) between the band-gap pressure coefficients of AlAs and GaAs, $a_p^{\Gamma-\Gamma}$ will decrease initially as AlAs composition increases. *Linear* extrapolation from the Al-poor samples has the tendency of underestimating $a_p^{\Gamma-\Gamma}$ (AlAs), thus, partially explains the experimental observation.¹⁹ Bowing of the band-gap pressure coefficient has also been noticed in³ $\text{Ga}_{0.5}\text{In}_{0.5}\text{P}$ and in⁴¹ $\text{GaN}_x\text{As}_{1-x}$ alloys. In fact, due to wave function mixing at the band edge, we expect that bowing of the pressure coefficient should be a common phenomena, especially for alloys whose constituents has large valence-band offset (e.g., MgSe and ZnSe) and/or large size mismatch (e.g., GaAs and GaN).

VI. LDA CORRECTED BAND-GAP PRESSURE COEFFICIENTS

LDA calculation underestimates the band-gap pressure coefficient, as seen in Table III and other first-principles calculations.⁴² To corrected the LDA error, we have adopted a simple method by adding an external potential^{42,43} to the LDA potential in solving the self-consistent LDA Schrodinger equations, so that the corrected band gaps are similar to experimental data⁶ or quasiparticle results.^{44,45} The LDA corrected band-gap deformation potentials and pressure coefficients for the group-IV, III-V, and II-VI compounds are given in Table V. The pressure coefficients are obtained using Eq. (3) and experimental bulk moduli given in Table II. The uncertainty of our predicted values is about 0.5 meV/kbar, mainly due to the uncertainty in fitting the external potentials and uncertainty of the experimental bulk moduli used to derive the pressure coefficients. We see that after correcting the LDA error in the band structure, the predicted values of a_p^α are in better agreement with experimental data (Table III). But the chemical trends are the same as in the LDA calculations.

VII. CONCLUSION

In summary, we have tested the validity of the ‘‘empirical rule’’ and studied the *chemical trends* of the band-gap pressure coefficients of all group IV, III-V and II-VI semiconductors. We also calculate the absolute deformation potentials of the VBM and CBM. We find that the volume deformation potentials a_v^{VBM} are small and negative for compounds containing occupied valence d state but positive for compounds without occupied valence d orbitals. Regarding the chemical trends of the band-gap pressure coefficients, we find that (i) $a_p^{\Gamma-\Gamma}$ decreases as the ionicity increases, (ii) $a_p^{\Gamma-\Gamma}$ increases significantly as anion atomic number in-

TABLE V. LDA-corrected band-gap volume deformation potentials (in eV) and pressure coefficient (in meV/kbar) of the three main transitions $\Gamma_{8v} \rightarrow X_{6c}$, $\Gamma_{8v} \rightarrow L_{6c}$, and $\Gamma_{8v} \rightarrow \Gamma_{6c}$ for group IV, III-V, and II-VI semiconductors. The pressure coefficients are obtained using Eqs. (1)–(3) and experimental bulk moduli of Table II.

Compound	$a_v^{\Gamma-X}$	$a_p^{\Gamma-X}$	$a_v^{\Gamma-L}$	$a_p^{\Gamma-L}$	$a_v^{\Gamma-\Gamma}$	$a_p^{\Gamma-\Gamma}$
C	-3.12	0.7	-14.77	3.3	-24.77	5.6
Si	1.35	-1.4	-4.07	4.2	-12.44	12.7
Ge	0.49	-0.7	-4.00	5.8	-10.06	14.6
Sn	0.46	-1.0	-2.71	5.9	-7.58	16.6
AlN	-1.13	0.5	-9.89	4.6	-10.16	4.7
AlP	1.34	-1.6	-4.38	5.1	-9.52	11.1
AlAs	1.01	-1.3	-4.60	5.9	-8.93	11.4
AlSb	1.18	-2.1	-3.64	6.6	-8.85	16.1
GaN	-1.21	0.6	-8.15	4.0	-7.37	3.6
GaP	1.27	-1.4	-3.83	4.3	-8.83	10.0
GaAs	1.05	-1.4	-3.70	4.9	-8.15	10.8
GaSb	1.12	-2.0	-3.06	5.4	-8.01	14.2
InN	-1.35	0.9	-5.23	3.5	-3.66	2.5
InP	1.00	-1.4	-3.00	4.2	-5.93	8.4
InAs	0.92	-1.6	-2.89	5.0	-5.66	9.8
InSb	1.10	-2.3	-2.51	5.2	-6.35	13.1
ZnS	1.09	-1.4	-3.09	4.0	-5.16	6.7
ZnSe	1.36	-2.2	-2.92	4.7	-4.99	8.0
ZnTe	1.72	-3.4	-2.40	4.7	-5.60	11.0
CdS	0.88	-1.4	-2.23	3.6	-2.94	4.7
CdSe	1.03	-1.9	-2.19	4.1	-2.90	5.5
CdTe	1.44	-3.2	-1.88	4.2	-3.70	8.3
HgS	1.32	-1.9	-1.10	1.6	-2.16	3.2
HgSe	1.56	-3.1	-0.90	1.8	-2.15	4.3
HgTe	1.97	-4.7	-0.74	1.8	-3.19	7.5

creases, (iii) $a_p^{\Gamma-\Gamma}$ decreases slightly as cation-atomic number increases, (iv) the variation of $a_p^{\Gamma-L}$ are relatively small and follow similar trends as $a_p^{\Gamma-\Gamma}$, and (v) the magnitude of $a_p^{\Gamma-X}$ are small; $a_p^{\Gamma-X}$ are usually negative, but are positive for compounds containing first-row elements (C, AlN, GaN, and InN). We suggest that the ‘‘empirical rule’’^{1,2} of the pressure coefficients should be modified and that one should be cautious in using the absolute deformation potentials from previous calculations.^{15,16}

ACKNOWLEDGMENTS

We thank Professor P. Y. Yu for raising our interest in this subject and many helpful discussions. This work was supported in part by the U.S. Department of Energy, Grant No. DE-AC36-98-GO-10337.

¹See review by W. Paul, *Proceedings of the International Symposium on Physical Properties of Solids Under High Pressure* (CERN, Paris, 1970), p. 199, and references therein.

²W. Paul, in *High Pressure in Semiconductor Physics*, edited by T. Suski and W. Paul, (Academic, San Diego, 1998), p. 1.

³A. Franceschetti and A. Zunger, *Appl. Phys. Lett.* **65**, 2990 (1994).

⁴See, for example, J. Chadi, and K. J. Chang, *Phys. Rev. Lett.* **61**, 873 (1988).

⁵See, for example, S. H. Kwok, P. Y. Yu, K. Uchida, and T. Arai,

- Appl. Phys. Lett. **71**, 1110 (1997).
- ⁶Numerical Data and Functional Relationships in Science and Technology, edited by O. Madelung and M. Schulz, Landolt-Bornstein, New Series, Group III, Vol. 22 Pt. a (Springer-Verlag, Berlin, 1987). See also Vol. 17, Pts a and b.
- ⁷A. D. Prins, J. L. Sly, and D. J. Dunstan, Phys. Status Solidi B **198**, 57 (1996).
- ⁸H. Teisseyre, B. Kozankiewicz, M. Leszczynski, I. Grzegory, T. Suski, M. Bockowski, S. Porowski, K. Pakula, P. M. Mensz, and I. B. Bhat, Phys. Status Solidi B **198**, 235 (1996).
- ⁹P. E. Van Camp, V. E. Van Doren, and J. T. Devreese, Phys. Rev. B **41**, 1598 (1990), and references therein.
- ¹⁰K. Reimann, M. Haselhoff, St. Rubenacke, and M. Steube, Phys. Status Solidi B **198**, 71 (1996).
- ¹¹J. Gonzalez, F. V. Perez, E. Moya, and J. C. Chervin, J. Phys. Chem. Solids **56**, 335 (1995).
- ¹²B. Gil and D. J. Dunstan, Semicond. Sci. Technol. **6**, 428 (1991).
- ¹³M. Zigone, H. Roux-Buisson, H. Tuffigo, N. Magnea, and H. Mariette, Semicond. Sci. Technol. **6**, 454 (1991).
- ¹⁴R. Resta, Phys. Rev. B **44**, 11 035 (1991).
- ¹⁵M. Cardona and N. E. Christensen, Phys. Rev. B **35**, 6182 (1987).
- ¹⁶C. G. Van de Walle, Phys. Rev. B **39**, 1871 (1989).
- ¹⁷A. Franceschetti, S.-H. Wei, and A. Zunger, Phys. Rev. B **50**, 17 797 (1994).
- ¹⁸D. Gershoni, C. H. Henry, and G. A. Baraff, IEEE J. Quantum Electron. **29**, 2433 (1993).
- ¹⁹S. Adachi, J. Appl. Phys. **58**, R1 (1985).
- ²⁰W. A. Harrison, *Electronic Structure and Properties of Solids* (Freeman, San Francisco, 1980).
- ²¹A. Zunger, Phys. Rev. Lett. **54**, 849 (1985); M. Caldas, A. Fazzio, and A. Zunger, Appl. Phys. Lett. **45**, 671 (1984); A. Zunger, Solid State Phys. **39**, 275 (1986).
- ²²D. D. Nolte, W. W. Walukiewicz, and E. E. Haller, Phys. Rev. Lett. **59**, 501 (1987).
- ²³W. W. Walukiewicz, J. Appl. Phys. **59**, 3577 (1987).
- ²⁴P. Hohenberg and W. Kohn, Phys. Rev. B **136**, B864 (1964); W. Kohn and L. J. Sham, *ibid.* **140**, A1133 (1965).
- ²⁵S.-H. Wei and H. Krakauer, Phys. Rev. Lett. **55**, 1200 (1985), and references therein.
- ²⁶D. M. Ceperly and B. J. Alder, Phys. Rev. Lett. **45**, 566 (1980).
- ²⁷J. P. Perdew and A. Zunger, Phys. Rev. B **23**, 5048 (1981).
- ²⁸D. J. Chadi and M. L. Cohen, Phys. Rev. B **8**, 5747 (1973).
- ²⁹F. D. Murnaghan, Proc. Natl. Acad. Sci. USA **30**, 244 (1944).
- ³⁰T. Kobayashi, T. Tei, K. Aoki, K. Yamamoto, and K. Abe, J. Lumin. **24-25**, 347 (1981).
- ³¹H. Muller, R. Trommer, M. Cardona, and P. Vogl, Phys. Rev. B **21**, 4879 (1980).
- ³²N. E. Christensen and I. Gorczyca, Phys. Rev. B **50**, 4397 (1994); B. A. Weinstein, P. Perlin, N. E. Christense, I. Gorczyca, V. Iota, T. Suski, P. Wisniewski, M. Osinski, and P. G. Eliseev, Solid State Commun. **106**, 567 (1998).
- ³³S.-H. Wei and A. Zunger, Phys. Rev. Lett. **59**, 144 (1987).
- ³⁴S.-H. Wei and A. Zunger, Phys. Rev. B **37**, 8958 (1988).
- ³⁵R. Resta, L. Colombo and S. Baroni, Phys. Rev. B **41**, 12 358 (1990).
- ³⁶W. R. L. Lambrecht, Phys. Rev. B **44**, 3685 (1991).
- ³⁷N. E. Christensen, in *High Pressure in Semiconductor Physics*, edited by T. Suski and W. Paul (Academic, San Diego, 1998), p. 49.
- ³⁸M. L. Cohen, Phys. Rev. B **32**, 7988 (1985); P. K. Lam, M. L. Cohen, and G. Martinez, *ibid.* **35**, 9190 (1987).
- ³⁹S. Fahy, K. J. Chang, S. G. Louie, and M. L. Cohen, Phys. Rev. B **35**, 5856 (1987).
- ⁴⁰A. Zunger, S.-H. Wei, L. G. Ferreira, and J. E. Bernard, Phys. Rev. Lett. **65**, 353 (1990); S.-H. Wei, L. G. Ferreira, J. E. Bernard, and A. Zunger, Phys. Rev. B **42**, 9622 (1990).
- ⁴¹T. Mattila, S.-H. Wei, and A. Zunger (unpublished).
- ⁴²N. E. Christensen, Phys. Rev. B **30**, 5753 (1984).
- ⁴³S.-H. Wei and A. Zunger, Phys. Rev. B **57**, 8983 (1998).
- ⁴⁴X. Zhu, S. Fahy, and S. G. Louie, Phys. Rev. B **39**, 7840 (1989).
- ⁴⁵O. Zakharov, A. Rubio, X. Blase, M. L. Cohen, and S. G. Louie, Phys. Rev. B **50**, 10 780 (1994).